Wireless Power Transfer under the Spotlight: Charging Terminals amid Dense Cellular Networks

Leonardo Bonati, Ángel Fernández Gambín, Michele Rossi
Dept. of Inf. Engineering (DEI), University of Padova, Italy

***Abstract*—Wireless Power Transfer (WPT) technology offers unprecedented opportunities to future cellular systems, making it possible to wirelessly recharge the mobile terminals as they get sufficiently close to the Base Stations (BSs). Here, we investigate the tradeoffs involved in the recharging process as multiple mobile users move across the cellular network, by systematically measuring the charging efficiency (i.e., amount of energy transferred as opposed to that transmitted) accounting for different mobility models, speeds, frequency range and inter-BS distance. We consider dense cellular deployments, where power is transferred to the mobile users through beamforming and scheduling techniques. At first, a genie is utilized to devise optimal charging schedules, where user locations and the residual energy in their batteries are exactly known by the controller. Hence, several heuristic policies are proposed and their performance is compared against that of the genie-based approach in terms of transfer efficiency and fraction of dead nodes (whose battery is completely depleted). Our numerical results reveal that: i) an even allocation of resources among users is inefficient, whereas even a rough estimate of their location allows heuristic policies to perform close to the genie-based approach, ii) mobility matters: group mobility leads to higher efficiencies and an increasing speed is also beneficial and iii) WPT can substantially reduce the number of dead nodes in the network, although this comes at the expense of constantly transmitting power and transfer efficiencies are very low under any scenario.**

***Index Terms*—Wireless Power Transfer, Energy Efficiency, Mobile Networks, 5G.**

I. Introduction

Nowadays, the Internet counts more than three billions active users in the world, sending more than two millions emails and watching more than 130 thousands YouTube videos per second [1]. The largest part of the overall Internet traffic is generated by mobile devices, which have almost completely replaced desktop computers and even laptops, to a large extent. These devices, either being smartphones, tablets or wearable ones, are battery-powered and tend to discharge quite rapidly. This fact usually forces their owners to plug them into power outlets during the day, maybe just for a short period of time, to gain that extra energy that permits the devices to safely reach the end of the day, when they will be plugged back in and be fully recharged. However, connecting a device to an energy source in the middle of the day is not always possible, due to the fact that the mobile user has to move from one place to another, or simply forgets the charger at home.

Wireless Power Transfer (WPT) [2] is a recent technique that allows charging a mobile device without the need to connect it to any external power supply and, in some cases, without the user even being aware of it. This technique relies on external tools, such as Base Stations (BSs) that are capable of communicating with the User Equipment (UE) and charging it by wirelessly sending power to it, if necessary. This approach involves a transmitter, i.e., a BS that sends power through the wireless medium, and at least one receiver, i.e., a UE that harvests this power to replenish its battery.

In this paper, we investigate the tradeoffs involved in the recharging process for a dense (e.g., inter-BS distances of about 20 meters) cellular network deployment, where mobile users can be wirelessly recharged through radio frequency transmissions. Our objective is to devise and systematically compare several distributed charging schemes, which dictate *which* users have to be charged and *when*, depending on the residual energy level in their batteries, on their distance from the serving BS, on the radiating frequency and on their mobility behavior. Most of the related literature focuses on a single BS that transmits power to the users being served, designing techniques that entail the joint transmission of power and information (see Section II). A distinctive trait of our work is that we look at a *distributed network deployment* and explicitly consider *user mobility*. We do not consider the transmission of information, but we are rather concerned with the allocation of power transfer slots from each BS according to the mobility patterns of the users and to the residual energy in their batteries. Our results shed some light on the actual effectiveness of WPT in future mobile networks, assessing whether it can be considered an effective means to charge terminals while they are on-the-go, considering real world system parameters, along with independent and group mobility models. Also, we provide useful results on the best WPT scheduling strategies. A somewhat counterintuitive finding from our study, is that the location of the mobile users is the sole metric that has to be taken into account in the design of WPT schedules, as this will steer the system toward higher transfer efficiencies and, at the same time, decrease the number of dead nodes. Designing for the battery level will lead to worse results in all respects.

In our numerical analysis, a genie is at first utilized to devise optimal charging schedules, where user locations and residual battery levels are exactly known by the BS controllers at all times. Hence, several heuristic policies are proposed and their performance is compared against that of genie-based approaches in terms of transfer efficiency and fraction of dead nodes (whose battery is completely depleted). Our results reveal that: i) an even allocation of resources among

978-1-5386-2723-5/17/$31.00

UEs is inefficient, whereas even a rough estimate of their location allows heuristic policies to perform very close to the genie-based schemes, ii) mobility matters: group mobility leads to higher efficiencies and an increasing speed is also beneficial, iii) wireless charging can substantially reduce the fraction of dead nodes, due to their battery level dropping below a certain critical threshold. Nevertheless, this comes at the expense of constantly transmitting power and transfer efficiencies are low under any scenario.

A final discussion on existing wireless charging techniques is in order. In the literature, three main approaches can be identified [2]: *1) Magnetic Inductive Coupling* is based on magnetic field induction, which exploits two aligned coils, one at the transmitter and the other one at the receiver, to transfer power, which is then converted into electrical energy. At the transmitter, a primary coil of conductive material is connected to an Alternating Current (AC) power source and generates an oscillating magnetic field. At the receiver, a secondary coil, close to the primary one, experiences an oscillating magnetic flux. Variations in this flux traversing the secondary coil induce an electric current, that can be used to charge a device's battery. *2) Magnetic Resonance Coupling* is based on evanescent-wave coupling, i.e., the coupling between two waves due to physical overlap, which, through varying or oscillating magnetic fields, generates and transfers power between two resonant coils, turned, then, into electrical energy. At the transmitter side, once the applied voltage triggers the oscillation, the circuit keeps resonating back and forth without consuming any additional energy [3]. *3) Microwave Radiation* exploits Radio Frequency (RF) waves to carry radiant energy [2]. The transmitter first performs an AC/DC conversion and then a DC/RF one through a magnetron, i.e., a vacuum tube which generates microwaves, when stimulated by a current. These are propagated through the air and captured, at the receiver side, by a rectenna, that converts them into Direct Current (DC) electricity. Microwaves can radiate energy in all directions isotropically, making them ideal for broadcast applications, or toward a specific one through beamforming, for point-to-point transmission. This last approach, called *transmit power beamforming*, can greatly improve the transmission efficiency and will be used in this work. Microwave radiation can reach longer distances than the previously described methods, and, through a low-power and long-distance transfer, it is capable of powering a large number of devices using a small amount of energy [4]. It is also compatible with existing communication systems [2] and can transfer both power and information at the same time using an approach called Simultaneous Wireless Information and Power Transfer (SWIPT) [5]. To this purpose, the amplitude and phase of microwaves are used to modulate information, while their radiation and vibration are used to carry energy [6]. This technique is deemed the most suitable for cellular networks.

The rest of the paper is organized as follows. In Section II, we discuss the related literature. Section III describes the system model. Then, WPT policies are proposed in Section IV. In Section V we present and discuss some selected numerical results. Finally, we conclude our work in Section VI.

II. Related Work

In an early work [7], the authors show that it is possible to apply WPT with satisfactory results. There, they wirelessly transferred power between a pair of devices by adopting self-resonant coils in a strongly coupled regime. The efficiency of the non-radiative transfer is demonstrated over higher distances than the radii of the two coils. A quantitative model, describing WPT, is also presented and the practical applicability of the system is discussed. It is also highlighted that specific materials and more elaborated geometries can be taken into account in order to improve the transfer efficiency. In this way, in [8], Kurs et al. exploit strongly coupled electromagnetic resonators to transfer power from a transmitter to a receiver separated by a distance much larger than the size of the resonators. This technique can also be used to remotely power multiple devices from a single transmitting source. The power transfer efficiency is experimentally shown for cases involving coupling objects of different sizes. The authors also highlight that a single source powering many small devices, distributed over a large volume, achieves a good overall efficiency, even in scenarios where the transfer efficiencies of the single devices are quite low.

In [6], the SWIPT approach, that not only transfers power, but also information content at the same time, was proposed. The authors studied the tradeoff between the rates at which energy and information can be injected over a wireless channel affected by noise. A capacity-energy function of the channel was also found. According to this paper, by adopting the found tradeoff, it is possible to receive both large amounts of energy and information per unit time. Moreover, a three-node wireless Multiple Input Multiple Output (MIMO) broadcasting system for SWIPT is described in [5], involving two receivers and a single transmitter. In the described scenario, one of the two receiving devices harvests energy from the source, while the other one decodes the transmitted information. Two cases are studied: one where the information and energy receivers see two different channels from the transmitter, and another one in which they see the same channel. In the first case, strategies for maximum information rate versus energy transfer are derived. In the second case, instead, a performance bound outside of the rate-energy region is shown. This bound, though, is not reachable with existing technology, because circuits for harvesting energy from radio signals are not able to also decode information yet.

In [9], an optimal packet scheduling problem in a single-user energy harvesting wireless communication system is considered. In this network scenario, both the data packets and the harvested energy are modeled at the source node as random arrival processes, and the goal is to adaptively change the transmission rate according to the traffic load and to the available energy, such that the time by which all packets are delivered is minimized. Moreover, the authors of [10] propose an amplify-and-forward relay network, where an energy constrained relay node harvests energy from an acquired RF

signal and uses it to forward the received information from the source to the destination.

The use of MIMO techniques along with beamforming allows for a considerable improvement in the transfer efficiency of energy and information. In [3], a MIMO beamforming scheme is considered to power mobile devices without needing them to be placed on apposite charging pads or with a particular orientation. This approach transfers power by beamforming the nonradiated magnetic field and steering it toward the mobile device. Differently to what is doable using traditional inductive or resonating techniques, where the device to be charged has to be placed close to the charger, with this scheme a UE can be charged while inside the owner's pocket or a bag. Also, it does not require to modify the smartphones' hardware, but can be used with today's devices by simply including a small receiver coil and circuit in a sleeve attached to the mobile device. A similar approach is presented in [11], where the authors consider a Multiple Input Single Output (MISO) femtocell cochannel overlaid with a Macrocell to exploit the advantages of SWIPT, while promoting the energy efficiency. The femto BSs send information and simultaneously transfer energy to femto users via beamforming.

Finally, a recent work [12] presents a model for joint downlink and uplink transmission of K-tier heterogeneous cellular networks with SWIPT for efficient spectrum and energy utilization. In the downlink transmission, mobile users, equipped with power splitting receiver architecture, simultaneously decode information and harvest energy. In the uplink transmission, instead, UEs use the harvested energy to transmit information.

The distinctive trait of our present work is that we explicitly consider user mobility in a distributed cellular system composed of several WPT-enabled BSs, investigating how mobility affects the charging efficiency of genie-based and heuristic (lightweight) approaches.

III. System Model

We consider a cellular network covering a toroidal area of $M_1 \times M_2$ square meters. Within such an area, we randomly deploy $N > 0$ nodes, that represent the UEs in the network, as well as $B > 0$ BSs, with $B \ll N$. Each base station $i = 0, \ldots, B-1$ keeps track of the nodes that are located inside its coverage area A_i and, each node $n = 0, \ldots, N-1$, keeps track of all the surrounding base stations. Hence, each node will be associated with the BS that provides the highest Received Signal Strength Indicator (RSSI), which is referred to as the *serving* BS. For WPT, each BS uses $M \geq 1$ transmitting antennas, whereas each UE uses a single antenna, entailing a MISO power transfer channel. The UEs are free to move according to a certain mobility model, whose discussion is deferred to Section III-D. In the following, we consider a target UE that is to be charged in a specific time slot by its serving BS and with d we mean their physical distance.

A. Channel Models

As for the channel model, we consider path loss and multi-path fading propagation phenomena. To model the path loss, we use the following simplified formula [13]: $P_{\mathrm{rx}} = P_{\mathrm{tx}} K (d_0/d)^{\gamma}$, where P_{tx} is the power transmitted by the BS, P_{rx} is the power received at the UE, d_0 is a reference distance for the antenna far-field, d is the distance between the WPT transmitter and the receiver, and γ is the path loss exponent. K depends on the antenna characteristics and is given by $K = (\lambda/(4\pi d_0))^2$, where λ is the wavelength. The power gain due to path loss is thus $f_{\mathrm{pl}}(d) = K(d_0/d)^{\gamma}$.

Furthermore, for the considered dense network scenario, which is typical of network deployments in urban areas, we assume that a direct channel between the BS and the UE is unlikely to exist and for this reason the UEs receive a number of weak multi-path components, whereas the direct path is blocked. In such case, the received fading envelope is Rayleigh distributed. In order to model the Rayleigh fading, we use an improved version of the Pop-Beaulieu simulator based on Clarke's model [14]. According to this model, the normalized lowpass fading process $y(t) = y_c(t) + j y_s(t)$ is obtained through a sum-of-sinusoids statistical simulation model, where:

$$y_c(t) = \frac{1}{\sqrt{P}} \sum_{p=1}^{P} \cos(\omega_d t \cos \alpha_p + \phi_p), \tag{1}$$

$$y_s(t) = \frac{1}{\sqrt{P}} \sum_{p=1}^{P} \sin(\omega_d t \cos \alpha_p + \phi_p), \tag{2}$$

with $\alpha_p = (2\pi p + \beta_p)/P$, $p = 1, 2, ..., P$, where P is the number of propagation paths, $\omega_d = 2\pi f_d$, f_d is the Doppler frequency, α_p and ϕ_p respectively represent the arrival angle (at the receiver) and the initial phase of the p-th propagation path. Finally, β_p and ϕ_p are statistically independent and uniformly distributed in $[-\pi, \pi)$, for all $p = 1, 2, \ldots, P$.

B. Transmission Beamforming for WPT

In the considered MISO scenario, beamforming techniques are utilized to increase the received power at the target UE. Here, we assume the channel gains are known at the transmitter and we use transmit beamforming [13] to maximize the amount of power that is transferred to the UE that is to be charged in the current time slot t. At the transmitter, the signal $s_i(t)$ that is to be transmitted from antenna i is multiplied by a complex gain $\omega_i = \rho_i e^{-j\theta_i}$, $\rho_i \in [0, 1]$. This multiplication implements co-phasing (θ_i) and weighting (ρ_i) relative to the channel gains. Let $g_i = \sqrt{f_{\mathrm{pl}}(d)} y(t)$ be the complex lowpass channel gain (amplitude domain) between the i-th antenna at the BS and the receiving antenna at the UE, which depends on the path loss gain $\sqrt{f_{\mathrm{pl}}(d)}$ and on the lowpass fading envelope $y(t)$ in the current time slot t. With perfect channel knowledge, co-phasing amounts to setting $\theta_i = \arg(g_i)$, $i = 1, \ldots, M$. Moreover, the combined lowpass signal at the receiver is:

$$r(t) = \sum_{i=1}^{M} \rho_i r_i s_i(t), \tag{3}$$

where $r_i = |g_i|$. For maximum power transfer, the (optimal) beamforming weights are obtained as [13]:

$$\rho_i = \frac{r_i}{\sqrt{\sum_{i=1}^{M} r_i^2}}, \tag{4}$$

which satisfies $\sum_{i=1}^{M} \rho_i^2 = 1$. With transmit beamforming and M transmit antennas at the BS, the power transmitted from antenna $i = 1, \ldots, M$, is $P_{\text{tx}}^i = P_{\text{tx}} \rho_i^2$, where P_{tx} is the total transmitted power. The harvested power Q at the target UE in slot t is proportional to the total received power in that slot, and is obtained as [11]:

$$Q = \xi \sum_{i=1}^{M} P_{\text{tx}} |g_i \omega_i|^2 = \xi P_{\text{tx}} \sum_{i=1}^{M} (\rho_i r_i)^2, \tag{5}$$

where $0 < \xi \leq 1$ is the power harvesting efficiency, which depends on the energy scavenging technology at the receiver. The channel gains g_i are obtained as a function of the path loss gain and of the multi-path fading envelope in the current time slot t. Moreover, we assume independently distributed fading processes across the transmitting antennas.

C. Energy Consumption and Efficiency Metrics

Time is slotted, slot times have a constant duration of T seconds, are grouped into windows, and each window contains W subsequent time slots. In each time slot, each UE consumes a certain power, P_d, which depends on the current task, i.e., emailing, Web browsing, calling, idling, etc. Assuming a constant power consumption in a time slot entails an energy drainage of TP_d.

The power consumption quantities, taken from [15], are measured using a Samsung Galaxy S3 smartphone and are shown in Table I. In our numerical results, one activity from this table is picked with a certain probability at the beginning of each time window and is kept unchanged for its whole duration. The energy consumption for a time window is thus $E_d = WTP_d$. Taking a specific UE $n = 0, \ldots, N-1$, and referring to its battery level at the beginning of window $w = 0, 1 \ldots$ as $E_{n,w}$, from window $w-1$ to w we have:

$$E_{n,w} = \begin{cases} E_{n,w-1} - E_{n,d} + E_{\text{rx},n,w-1}, & \text{if } E_{n,w} > 0 \\ 0, & \text{otherwise,} \end{cases} \tag{6}$$

where $E_{n,d}$ is the energy consumed by UE n due to the phone's activity and $E_{\text{rx},n,w-1}$ is the energy harvested by this user through WPT in window $w-1$. Note that, if the battery gets empty, i.e., $E_{n,w} = 0$, UE n is considered *dead* and cannot be wirelessly charged any longer.

WPT efficiency: for a given WPT scheduling policy, we measure the wireless power transfer efficiency $\eta \in [0, 1]$ as the ratio between the total energy harvested by the UEs and the total amount of energy that is transmitted by the BSs:

$$\eta = \lim_{L \to +\infty} \frac{\sum_{w=0}^{L-1} \sum_{n=0}^{N-1} E_{\text{rx},n,w}}{\sum_{w=0}^{L-1} \sum_{i=0}^{B-1} E_{\text{tx},i,w}}, \tag{7}$$

where L is the number of time windows, B is the number of BSs, N is the number of UEs, $E_{\text{tx},i,w}$ and $E_{\text{rx},n,w}$ respectively represent the total energy transmitted by BS i and the total energy harvested by UE n within time window w.

TABLE I
BATTERY DISCHARGE POWER P_d *vs* ACTIVITY FROM [15].

Task	P_d [mW]
Audio	226
Email	1299
Phone call	854
Standby	24
Web	1080

Charging metrics: at the beginning of a new window w, each BS i has to decide which ones of the users within its own coverage area A_i are to be charged and in which time slots: this is referred to as *power transfer schedule*. This decision is made in order to maximize one of the following global metrics. *Metric 1* (M_1) jointly considers the transfer efficiency η and the residual battery level averaged over all UEs across all time slots, E, and is obtained by their linear combination through a weight $\alpha \in [0, 1]$:

$$M_1 = \alpha \eta + (1 - \alpha) E. \tag{8}$$

Here, $\alpha \in [0, 1]$ weighs the importance of the charging efficiency versus the residual energy level of the terminals. In fact, when $\alpha = 1$ the UEs providing the best transfer efficiency (i.e., the highest η) are charged, as these will have the largest M_1 metric, while when $\alpha = 0$ the devices whose battery is about to deplete are prioritized, as charging these will increase E. Intermediate cases occur for $0 < \alpha < 1$.

With *Metric 2* (M_2), the previous quantities are multiplied:

$$M_2 = \eta E. \tag{9}$$

Here, the UEs with the lowest battery level, and that at the same time would benefit the most from the power transfer (leading to the highest η), are prioritized.

In the charging strategies that will be discussed in Section IV, we aim at maximizing the global metrics M_1 and M_2 by devising WPT schedules on a window-by-window basis. That is, at the beginning of any time window $w = 0, 1, \ldots$, each BS assesses the η and E metrics only for the users within its cell and for the entire window w. The best local schedule is then found through dynamic programming, by assessing all the possible allocation policies for the W time slots in the current window w [16]. The policies that we obtain through this approach are referred to as *genie-based* in Section IV, are

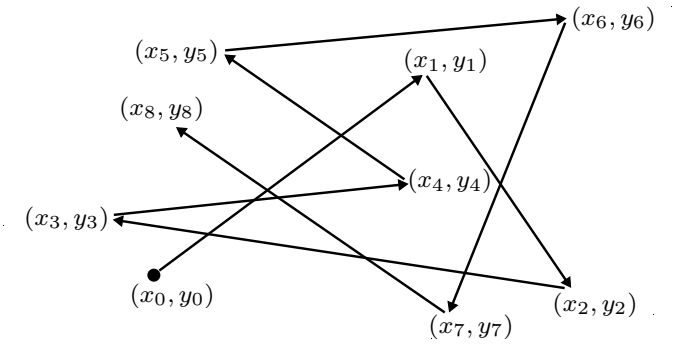

Fig. 1. Example of node's movement in RWP [19]. (x_i, y_i), $i \in \{1, \ldots, 8\}$, are the destinations for 8 subsequent steps, (x_0, y_0) is the initial position.

not guaranteed to lead to the globally optimal metrics, but are preferred due to their practical and lightweight character.

D. Mobility Models

For the mobility, we consider the Random Waypoint Model (RWP) and Reference Point Group Mobility Model (RPGM).

RWP allows the users to move freely and without restrictions around the network. In this model, first proposed by Johnson and Maltz [17], [18], UEs randomly choose their destination, speed and traveling direction and they do so independently of other users. RWP permits to study mobility scenarios where the users travel alone. At the beginning of the algorithm, each UE randomly chooses its destination and speed $\boldsymbol{v}$ such that its modulus is $|\boldsymbol{v}| \in [v_{\min}, v_{\max}]$, where $v_{\min}$ and $v_{\max}$ respectively are the minimum and maximum speed, then it chooses the movement direction in order to get closer to its destination. Upon reaching it, the user stops for a pause time T_{pause}, then he randomly chooses a new destination and the whole process repeats anew. A mobility path example for RWP is shown in Fig. 1.

RPGM [19], permits to study mobility scenarios where the movements of UEs are spatially correlated, i.e., users moving in groups, or carrying multiple devices. Nodes are divided into *group leaders* and *followers* and each group is composed of a group leader, that determines the direction of movement and speed for the whole group, and a certain number of followers, that tag along the leader of their group. At the beginning of the algorithm, each group leader behaves as an RWP node would do, i.e., randomly choosing his destination and speed and, at each round, he gets closer to his destination. The followers, instead, move in the same direction and with the same speed of their group leader, eventually deviating of a bounded distance from their reference point, i.e., the point they would reach traveling along the very same direction of their leader and with the same speed. This process goes on until the leader reaches his intended destination, then the whole group stops for a pause time, T_{pause}, after which the leader chooses another destination and the whole process repeats again. A group mobility example in RPGM is shown in Fig. 2.

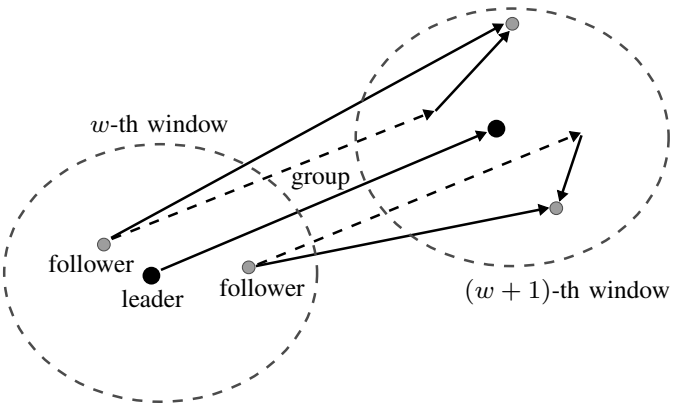

Fig. 2. Example of group movement in RPGM [19]. The dashed straight lines represent the followers' reference path in absence of deviations. Two topology snapshots are drawn: one at the w-th window, and one at the $(w+1)$-th window.

IV. Wireless Power Transfer Policies

Whenever the battery energy of any UE decreases below a certain threshold, $E_{\text{th}} \in (0, E_{\max}]$ ($E_{\max}$ is the UE's maximum battery energy), the UE sends a charging request to the BSs within coverage. The collection of charging requests and the decision of which UEs are to be charged is made on a window-by-window basis. Specifically, the requests that arrive during window $w-1$ are processed at the beginning of the w-th window, at which point the BSs decide which of the requesting users shall be charged during window w. Hence, a certain amount of power will be wirelessly transmitted to the selected users in their allotted time slots in a Time Division Multiple Access (TDMA) fashion. Note that the time slot allocation has to be made wisely, i.e., in order to maximize some selected metrics (see previous metrics M_1 and M_2). This means that, depending on the specific metric that is to be maximized, some users may be preferred as they are located within a shorter distance from the base station and thus the power transfer efficiency toward them is higher or other users may be given higher priority as their battery is about to deplete (i.e., energy level below E_{th}). Hence, in each window the number of time slots that is to be allocated by each BS to each user within coverage may change and may be uneven across different users, depending on their battery level and location. Next, we propose several policies to obtain suitable *power transfer schedules* by adopting genie or heuristic approaches and considering either metric M_1 or M_2.

A. Policy 1 (genie-based, metric M_1)

According to Policy 1 (P1), the BSs exactly know the position of all UEs throughout the entire simulation and optimally allocate TDMA (power transfer) time slots among the nodes that are to be charged, so as to maximize metric M_1 of Eq. (8).

Policy P1 uses a *genie* which knows the exact position of all users at all times. P1 is utilized as a benchmark for the *heuristic* policies that we detail below.

B. Policy 2 (heuristic, metric M_1)

With Policy 2 (P2), instead, the BSs estimate the positions of the UEs in the *current* time window. Any BS i, given that a UE is inside its coverage area A_i, and by observing at least two different positions of it, predicts its trajectory as we now describe. Consider UE $n \in \{0, \ldots, N-1\}$, and assume that we measure its position in time slots t and $t-k$, with $k \geq 1$, which we respectively call $\boldsymbol{p}_{n,t} = (p_{n,t,x}, p_{n,t,y})$ and $\boldsymbol{p}_{n,t-k} = (p_{n,t-k,x}, p_{n,t-k,y})$. The UE speed $\boldsymbol{v}_n = (v_{n,x}, v_{n,y})$ is then estimated as:

$$v_{n,x} = \frac{p_{n,t,x} - p_{n,t-k,x}}{Tk}, \tag{10}$$

$$v_{n,y} = \frac{p_{n,t,y} - p_{n,t-k,y}}{Tk}, \tag{11}$$

where T is the duration of a time slot. The BS can also estimate the future UE location at any time slot $t' > t$, $\hat{\boldsymbol{p}}_{n,t'} = (\hat{p}_{n,t',x}, \hat{p}_{n,t',y})$, as:

$$\hat{p}_{n,t',x} = p_{n,t,x} + v_{n,x}(t'-t)T, \tag{12}$$

$$\hat{p}_{n,t',y} = p_{n,t,y} + v_{n,y}(t'-t)T. \tag{13}$$

If BS i sees that the estimated future position of any UE n falls outside its coverage area, say, inside the one of BS j, with $i, j \in \{0, \ldots, B-1\}$, $i \neq j$, it notifies the latter BS of this fact, providing it with estimates of the UE arrival time and location. Given that each BS executes the above steps, estimates for UEs arrivals and departures are available to all BSs. After executing these estimations, which are made at the beginning of each window w, the BSs pick the power transfer slots as in P1, i.e., they determine the UEs to charge in order to maximize metric M_1 of Eq. (8) for each time slot. The only difference with respect to P1 is that in this case the estimated locations are used in place of the exact ones.

C. Policy 3 (genie-based, no metric)

With Policy 3 (P3) the BSs know the location of the UEs inside their coverage area A_i at the beginning of each time window. However, for the remaining time slots within the same time window they only know whether each of these UEs will remain inside their coverage area A_i. Hence, for any given time window, each BS $i = 0, \ldots, B-1$ only charges the UEs that have issued a charging request (with energy level below E_{th} at the beginning of the time window) and that remain inside its coverage area A_i for the entire window. For the charging schedule, the TDMA slots in the window are evenly split among these UEs. P3 is a *genie* policy as, although the exact position of the UEs is not known for all the future time slots, their serving BS is known beforehand for all the future slots in the current window, and since the beginning of it.

D. Policy 4 (heuristic, no metric)

With Policy 4 (P4), as with P3, the BSs only know the location of the UEs at the beginning of the current time window. Differently from P3, though, each BS i does not know those nodes that remain inside its coverage area A_i, but has to get an estimate for this using a method analogous to that of P2. After this, the TDMA time slots are evenly split among all the UEs that are estimated to remain within the coverage area A_i and that need to be charged, i.e., whose energy level is below E_{th} at the beginning of the time window.

E. Policy 5 (genie-based, metric M_2)

With Policy 5 (P5), the BSs exactly know the position of the UEs throughout the simulation and optimally allocate TDMA slots between the nodes to charge. Differently from P1, though, with P5 the BSs do this in order to maximize metric M_2, see Eq. (9). Analogously to P1, also P5 is a *genie* policy, designed to evaluate the performance of its corresponding heuristic policy, i.e., Policy 6 (P6).

F. Policy 6 (heuristic, metric M_2)

With P6, instead, each BS i has to estimate the future positions of the UEs inside its coverage area A_i and does so in the very same way as with P2. Differently from P2, though, the metric to maximize when choosing which UEs are to be charged is M_2, see Eq. (9).

V. Performance Evaluation

In this section, we present some selected numerical results for the WPT scenario of Section III. The parameters that were used for the simulations are given in the following Tables II and III. In all the graphs reported below, the network area is 1600 m^2 for an inter-BS distance of $d_{\text{BS}} = 20$ m, except for Fig. 3, where it varies according to d_{BS}.

In Fig. 3, we show the transfer efficiency η obtained by the considered policies P1-P6 for $N = 100$ users, $P_{\text{tx}} = 16$ W, $M = 4$, $v_{\max} = 2.5$ m/s and varying the inter-BS distance in $d_{\text{BS}} \in [20, 100]$ m. As expected, for all the policies, the transfer efficiency increases with a decreasing inter-BS distance. This confirms that a densely deployed scenario, such as the one envisioned for next generation mobile networks, is beneficial to WPT. Further, we see that P1, P2, P5 and P6 behave similarly for the whole range of distances, with P1 and P2 being respectively the best and second-best. This fact was consistently verified across the whole parameter range, which means that metric M_1 has to be preferred to M_2. We also observe that P3 and P4 provide unsatisfactory performance, and this indicates that the user location (or at least a good estimate of it) is a valuable information for the considered WPT scheduling task. The inadequacy of P3 and P4 has been confirmed in all our numerical results. For these reasons, P3, P4, P5 and P6 will be dismissed and will no longer be considered in the following plots.

In Fig. 4, we explore the relationship between the power transfer efficiency η and the transmit frequency f_{tx}. As expected, lower frequencies are to be preferred and those commonly used for FM broadcasting (around 100 MHz) provide the highest transfer efficiencies within the considered frequency range, due to their lower path loss. As promptly inferred from this plot, the transfer efficiency that we may expect from this technology is rather small, but as we shall see in the following, when the network deployment is dense

TABLE II
SYSTEM PARAMETERS USED IN THE NUMERICAL RESULTS.

Parameter	Value
BS coverage range	10 m
Power harvesting efficiency, ξ	0.4
Energy threshold to issue a charging request, E_{th}	30% of $E_{\max}$
Inter-BS distance, d_{BS}	$[20, 100]$ m
Minimum UE speed, $v_{\min}$	0 m/s
Maximum UE speed, $v_{\max}$	$[1, 4.5]$ m/s
Network area	$[1600, 40000]$ m^2
Number of antennas per BS, M	$[1, 8]$
Number of fading paths, P	8
Number of TDMA slots per window	10
Number of UEs, N	100
Number of UEs per group in RPGM	5
Number of windows in each simulation	28800
Path loss exponent, γ	3.5
Pause time, T_{pause}	2 s
Reference distance, d_0	1 m
Window duration	2 s
Total transmit power, P_{tx}	16 W
Transmit frequency, f_{tx}	$[100, 2000]$ MHz
UE battery capacity	2100 mAh
UE battery voltage	3.8 V

TABLE III
PARAMETERS USED IN THE FOLLOWING PLOTS.

Figure	α	d_{BS} [m]	f_{tx} [MHz]	M	$v_{\max}$ [m/s]
Fig. 3	1	$[20, 100]$	100	4	2.5
Fig. 4	1	20	$[100, 2000]$	4	2.5
Fig. 5	1	20	100	4	$[1, 4.5]$
Fig. 6	1	20	100	$[1, 8]$	2.5
Fig. 7	$[0, 1]$	20	100	4	2.5
Fig. 8	$[0, 1]$	20	100	4	2.5
Fig. 9	1	20	100	$[1, 8]$	2.5

(e.g., $d_{\text{BS}} = 20$ m) the mobile users may still be able to charge their batteries (although at a low pace) and a good percentage of them to prevent their batteries from draining fast or being depleted. Moreover, in Fig. 4 we show results for random (RWP) and group (RPGM) mobility and we see that group mobility attains the best transfer efficiencies. In fact, we observe that when one user is in a favorable location (i.e., close to a WPT-enabled BS), with high probability his followers will also be favorably located. Hence, more users will be efficiently charged per unit time than with RWP mobility. This was consistently verified across all our experiments.

Another interesting result is shown in Fig. 5, where we compare policies P1 and P2 for an increasing UE speed. From this plot, we see that mobility is actually beneficial in terms of η. This is because, through mobility, even users that are initially located far away from the WPT-enabled BSs eventually move closer to one of them and can thus benefit from WPT. Hence, the probability that there exist users in favorable

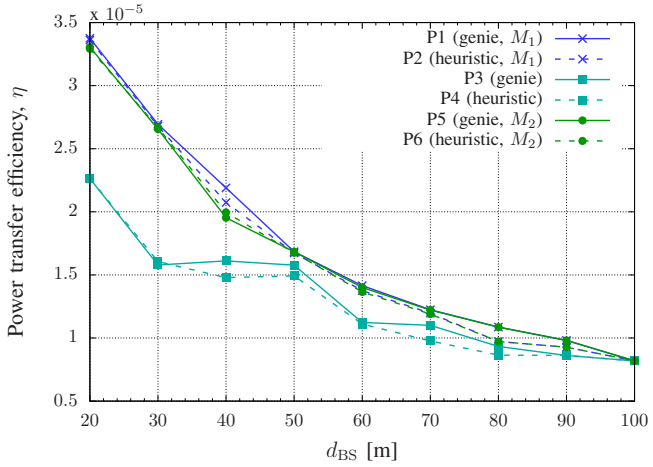

Fig. 3. Power transfer efficiency η *vs* inter-base station distance d_{BS}. RWP mobility, $N = 100$ UEs, $P_{\text{tx}} = 16$ W and $M = 4$ transmit antennas.

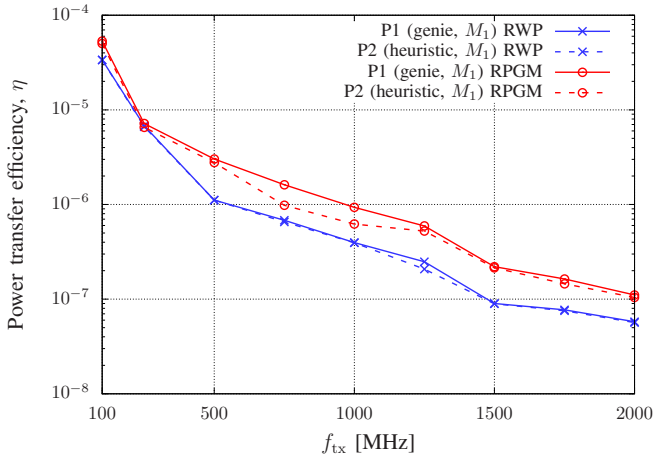

Fig. 4. Power transfer efficiency η varying the transmit frequency f_{tx}.

positions, i.e., close to some WPT-enabled BS is higher in the presence of mobility and increases with an increasing maximum speed $v_{\max}$. Although not shown in the plot for the sake of readability, the gap between P3/P4 and P1/P2 becomes substantial, which confirms that it is inappropriate to charge users without accounting for their distance from the charging BS. As for policies P5/P6, these still perform close to P1/P2, but their performance is always dominated. Also, an increasing speed leads to a higher gap between genie-based and heuristic policies and this is because the estimates obtained through Eq. (12) and (13) become less accurate. This is especially evident with RPGM mobility, as group mobility patterns are poorly described by these estimates (where the mobility of each terminal is independently assessed).

Fig. 6 shows the transfer efficiency η as a function of the number of transmit antennas M at the charging BS. When a single antenna is employed ($M = 1$, no beamforming) we obtain the lowest efficiency, which then improves by more than one order of magnitude for $M = 2$ and more than two for $M = 4$. Beyond $M = 4$, the additional improvement

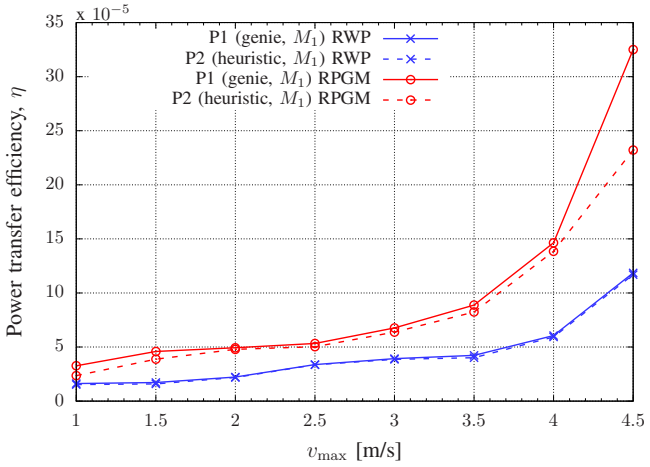

Fig. 5. Power transfer efficiency η varying the maximum UE speed $v_{\max}$.

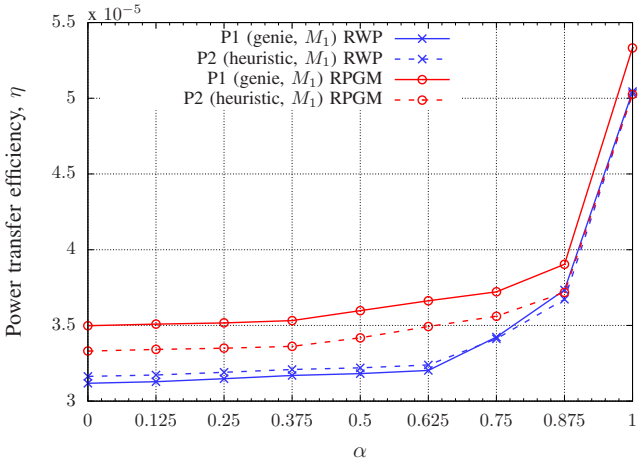

Fig. 7. Power transfer efficiency η *vs* α.

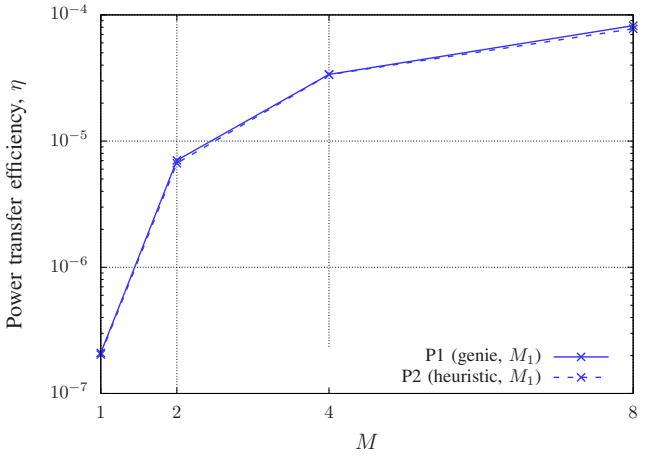

Fig. 6. Power transfer efficiency η *vs* number of transmit antennas, M.

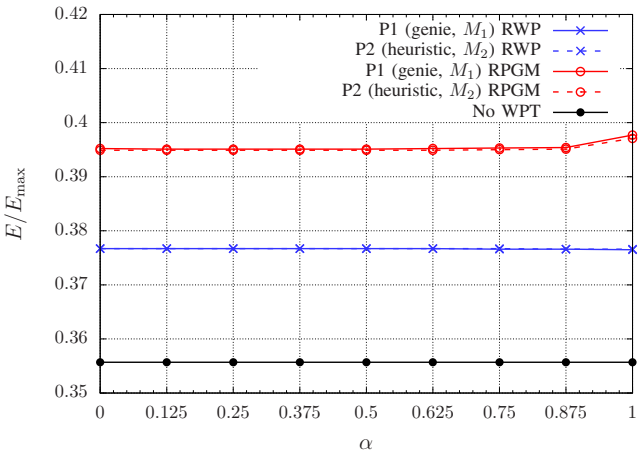

Fig. 8. Normalized average energy per non-dead node per window *vs* α.

is marginal. We observe that, in theory, additional benefits may be possible by also using antenna arrays at the receiver side. Due to space constraints at the UEs, this is however only feasible at high frequencies (in the GHz range), due to the antenna size and the separation ($\approx \lambda/2$) that is required to ensure uncorrelated fading among antennas. Nevertheless, in the GHz range the efficiency appears too small to justify the use of WPT in the considered network scenario (see Fig. 4).

In Fig. 7, we show the efficiency η for the best policies P1 and P2 as a function of the weight α (see Eq. (8)). With $\alpha = 1$, metric M_1 puts more weight on η, which becomes the only performance indicator to be maximized. As seen from this graph, this is in fact what the policies do: as α goes from 0 to 1, the efficiency η correspondingly increases of about 50%. In this figure, we also show the impact of the mobility behavior, plotting results for the RWP and RPGM mobility models. Once again, group mobility leads to the highest efficiencies.

At this point, one might rightly wonder what happens to the energy metric E when we decrease α down to 0. This latter tradeoff is shown in Fig. 8, from which we get a somewhat counterintuitive result, i.e., that putting more weight on the residual energy level at the nodes ($\alpha \to 0$) does not lead to an increased energy metric E, but the residual energy is actually maximized when $\alpha = 1$, i.e., when the WPT schedules are solely computed based on the power transfer efficiency η. The reason behind this is that, when $\alpha = 0$, WPT slots will be assigned based on the residual energy level and disregarding the users' location. However, with this approach it may happen that users that are located far away from the BSs will be charged anyway as their energy level is below threshold, but the charging efficiency in this case will be very small and we would be better off by charging these users as they get sufficiently close to one of the WPT-enabled BSs. Overall, this means that the best strategy is to compute the charging schedules only based on the UE location, as the transfer efficiency will otherwise be too small. Besides, Fig. 8 confirms the fact that group mobility helps increase the nodes' energy level and that the heuristic policy P2 for $v_{max} = 2.5$ m/s performs very close to the genie-based policy P1.

In the last Fig. 9, we evaluate the fraction of UEs whose

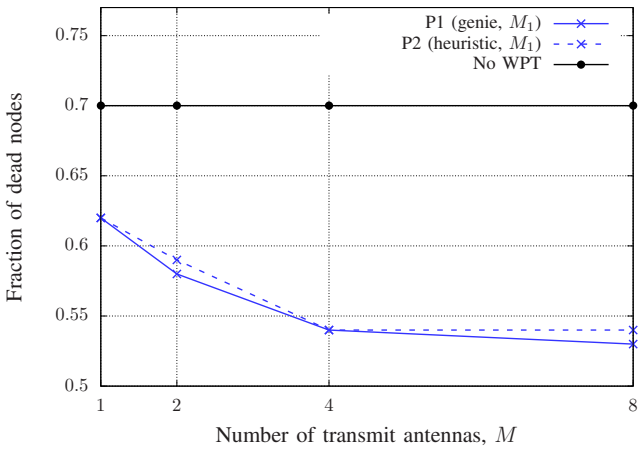

Fig. 9. Fraction of dead nodes *vs* number of transmit antennas M. RWP mobility with maximum user speed $v_{\max} = 2.5$ m/s.

battery is depleted during the simulation for a pedestrian mobility scenario ($v_{\max} = 2.5$ m/s). Once again, we see that beamforming is quite efficient, lowering this fraction from 0.7 (i.e., 70% of the users) down to 0.53 for $M = 8$, which corresponds to a relative improvement of about 24%. This is considerable, especially in light of the very small efficiencies that are provided by WPT in the considered network scenario. Although not evaluated in the present work, we foresee that in the near future BSs will be equipped with energy harvesting technology (e.g., solar panels), which will make it possible to collect ambient energy. Part of this energy, especially during daytime, could be used to charge mobile users. Although the charging efficiency is very low, this ancillary service is valuable to the users, who may be willing to pay for it, generating revenue for the mobile operators.

VI. Conclusions

In this work, we studied WPT techniques for next generation mobile networks, using transmit beamforming to wirelessly charge mobile UEs in densely-deployed MISO femtocell networks. We designed several policies, both genie-aided and heuristic, to assess which users are to be charged and in which time slots, while prioritizing them based on their location and on their battery level.

Through numerical simulation, we have then analyzed the performance of these policies finding that heuristic approaches, that estimate the user locations, behave surprisingly close to genie-aided ones, where locations are exactly known for all the future time slots. This is especially true for pedestrian scenarios, where the user speed is moderate and even simple linear approximations suffice to obtain accurate estimates. We have also assessed the impact of the mobility behavior, finding that mobility helps increase the power transfer efficiency and also that the best results are achieved when users move in groups. Although typical WPT efficiencies are rather small in any scenario, our results indicate that the number of dead nodes, whose battery is depleted during the simulation, decreases of about 24% with WPT for an inter-BS distance of 20 meters. As a future work, the case where BSs harvest ambient energy and use it to charge the UEs may be considered. In that setting, it would be interesting to see whether the amount of energy harvested still suffices to support the WPT service, getting the advantages that we have measured here.

Acknowledgment

This work has received funding from the European Union's Horizon 2020 research and innovation programme under the Marie Sklodowska-Curie grant agreement No 675891 (SCAVENGE).

References

[1] (2016, Dec) Internet Live Stats. [Online]. Available: http://www.internetlivestats.com/

[2] X. Lu, D. Niyato, P. Wang, D. I. Kim, and Z. Han, "Wireless charger networking for mobile devices: fundamentals, standards, and applications," *IEEE Wireless Communications*, vol. 22, no. 2, pp. 126–135, Apr 2015.

[3] J. Jadidian and D. Katabi, "Magnetic MIMO: How to Charge Your Phone in Your Pocket," in *Annual International Conference on Mobile Computing and Networking*, Maui, HI, US, Sept 2014.

[4] X. Lu, P. Wang, D. Niyato, and Z. Han, "Resource allocation in wireless networks with RF energy harvesting and transfer," *IEEE Network*, vol. 29, no. 6, pp. 68–75, Dec 2015.

[5] R. Zhang and C. K. Ho, "MIMO Broadcasting for Simultaneous Wireless Information and Power Transfer," in *IEEE Global Telecommunications Conference*, Houston, TX, US, Dec 2011.

[6] L. R. Varshney, "Transporting information and energy simultaneously," in *IEEE International Symposium on Information Theory*, Toronto, ON, CA, July 2008.

[7] A. Kurs, A. Karalis, R. Moffatt, J. D. Joannopoulos, P. Fisher, and M. Soljačić, "Wireless power transfer via strongly coupled magnetic resonances," *Science*, vol. 317, no. 5834, pp. 83–86, July 2007.

[8] A. Kurs, R. Moffatt, and M. Soljačić, "Simultaneous mid-range power transfer to multiple devices," *Applied Physics Letters*, vol. 96, no. 4, pp. 044 102:1–044 102:3, Jan 2010.

[9] J. Yang and S. Ulukus, "Optimal Packet Scheduling in an Energy Harvesting Communication System," *IEEE Transactions on Communications*, vol. 60, no. 1, pp. 220–230, Jan 2012.

[10] A. A. Nasir, X. Zhou, S. Durrani, and R. A. Kennedy, "Relaying Protocols for Wireless Energy Harvesting and Information Processing," *IEEE Transactions on Wireless Communications*, vol. 12, no. 7, pp. 3622–3636, July 2013.

[11] M. Sheng, L. Wang, X. Wang, Y. Zhang, C. Xu, and J. Li, "Energy Efficient Beamforming in MISO Heterogeneous Cellular Networks With Wireless Information and Power Transfer," *IEEE Journal on Selected Areas in Communications*, vol. 34, no. 4, pp. 954–968, Apr 2016.

[12] S. Akbar, Y. Deng, A. Nallanathan, M. Elkashlan, and A.-H. Aghvami, "Simultaneous Wireless Information and Power Transfer in K-Tier Heterogeneous Cellular Networks," *IEEE Transactions on Wireless Communications*, vol. 15, no. 8, pp. 5804–5818, Aug 2016.

[13] A. Goldsmith, *Wireless Communications*. New York, NY, US: Cambridge University Press, 2005.

[14] C. Xiao, Y. R. Zheng, and N. C. Beaulieu, "Novel Sum-of-Sinusoids Simulation Models for Rayleigh and Rician Fading Channels," *IEEE Transactions on Wireless Communications*, vol. 5, no. 12, pp. 3667–3679, Dec 2006.

[15] A. Carroll and G. Heiser, "The systems hacker's guide to the galaxy energy usage in a modern smartphone," in *ACM Proceedings of the 4th Asia-Pacific Workshop on Systems*, Singapore, Singapore, July 2013.

[16] E. V. Denardo, *Dynamic Programming: Models and Applications*. Mineola, NY, US: Dover Publications, 2003.

[17] J. Broch, D. A. Maltz, D. B. Johnson, Y.-C. Hu, and J. Jetcheva, "A performance comparison of multi-hop wireless ad hoc network routing protocols," in *ACM/IEEE international conference on Mobile computing and networking*, Dallas, TX, US, Oct 1998.

[18] D. B. Johnson and D. A. Maltz, *Dynamic Source Routing in Ad Hoc Wireless Networks*. Boston, MA, US: Springer US, 1996, pp. 153–181.

[19] F. Bai and A. Helmy, "A survey of mobility models," *Wireless Adhoc Networks*, vol. 206, pp. 147–176, June 2004.